Analysis and tuning methodology of FAPI controllers for maximising the share of grid-connected wind generations

Elyas Rakhshani[1] ✉, Arcadio Perilla[1], Nidarshan Veerakumar[1], Zameer Ahmad[1], Jose Rueda Torres[1], Mart van der Meijden[1,2], Peter Palensky[1]

[1]*Department of Electrical Sustainable Energy, Delft University of Technology, 2628 Delft, The Netherlands*

[2]*TenneT TSO B.V, Arnhem, The Netherlands*

✉ *E-mail: E.Rakhshani@tudelft.nl*

Abstract: In this study, a novel methodology is proposed for sensitivity-based tuning and analysis of derivative-based fast active power injection (FAPI) controllers in type-4 wind turbine units integrated into a low-inertia power system. The FAPI controller is attached to a power electronic interfaced generation (PEIG) represented by a generic model of wind turbines type 4. It consists of a combination of droop and derivative controllers, which is dependent on the measurement of the frequency. The tuning methodology performs parametric sensitivity to search for the most suitable set of parameters of the attached FAPI that minimises the maximum frequency deviation in the containment period. The FAPI is adjusted to safeguard system stability when increasing the share of PEIG. Since the input signal of the FAPI is the measured frequency, the impact of different values and parameter settings of the phase-locked loop used for the FAPI controller is also investigated. Detailed validation with a full-scaled wind power converter is also provided with a real-time digital simulator testbed. Obtained simulation results using a three-area test system, identify the maximum achievable degree of increase in the share of wind power when a proper combination of wind park locations considering their suggested settings for inertia emulation.

1 Introduction

Frequency stability depends on the ability to rapidly restore the equilibrium (within the time frame of frequency containment period which is the period after unbalancing occurrence up to 30 s) between system generation and load demand with minimum loss of loads. This ability can be limited especially in the modern systems with low inertia [1–4].

A low-inertia power system is a result of replacing conventional synchronous generators with a huge amount of power electronic interfaced generation (PEIG) units like solar photovoltaic systems and wind generation (WG) units [5–7]. The stochastic behaviour of renewable-based generation power plants might also deteriorate the dynamic performance of the system, especially during the contingencies. Thus, supplementary mitigation strategies such as the embedding additional energy storage systems (ESSs) with added controllers for enabling fast frequency response (FFR) or fast active power injection (FAPI) are needed to safeguard the system against undesirable frequency problems [6]. As it was mentioned, FAPI is a mechanism that can adjust the injection of active power through the source of the energy in a very fast manner for mitigating the frequency distortions in a system with a high share of renewables [7]. The required energy for providing inertial response can be provided using different power electronic interfaces, like ultracapacitor banks, batteries and rotating parts in wind turbines. A proper control strategy for such elements can enable the wind turbine for releasing the required energy to arrest the frequency deviations within 10 s [8, 9]. FAPI controllers can be classified in three main families, namely, droop-based controllers (proportional controllers) [7, 10, 11], derivative-based controllers [12–14], and other approaches which are based on a mathematical representation of swing equation of conventional synchronous generators, thus attempting to represent a virtual synchronous machine (VSM) for emulating inertia [15, 16].

As reported in [17], a high-order equation-based method for developing a VSM equation (VSME) has been proposed in [17]. The proposed coherency identification method is used for a DFIG-based wind power plant. The VSME in this reference shows high complexity as other VSM methods in terms of the number of equations and controller gains.

Thanks to technological advancement, a DC link-based inertia emulation approach with coordination of the modular multilevel converter based high-voltage DC (MMC-HVDC) link for wind power integration is presented and discussed in [18]. The method is very interesting and the required energy is provided from electrostatic energy stored within the cells of the DC link.

Different operational planning strategies for implementing virtual inertia control have been reported in [19, 20]. The proposed strategy in [19] is developed for the use of energy storage to limit the rate of change of frequency (RoCoF) within the acceptable thresholds in a power system with low-inertia capabilities. Thus, a suitable type of virtual inertia support coordinated with WG unit with an estimation of the required capacity for storage element is determined.

As reported in [21] accurate estimation of inertia can play a key role during the implementation of a virtual inertia controller. In this reference, an analysis of power system inertia estimation from frequency excursions is carried out by considering different inertia estimation methodologies for a system with a high share of wind power plants. It is suggested to use an accurate estimation methodology for inertia especially when a virtual inertia control, proportional- or derivative-based control, is used by a wind power plant.

As indicated in most of these references, proportional or derivative control is among the most common approaches for emulating virtual inertia. The controllers which are only based on the derivative approach alone might have some complications, which is due to its restriction with noise amplification [8]. The addition of droop-based control can be reflected as a complementary control loop for creating an additional reference signal for active power control block of the wind turbine which will be in proportion to the changes in the system's frequency. It can bring a better recovery response with more enhancements in Nadir [22–24]. Thus in this paper, the combination of both droop and derivative-based control techniques has been used for developing a new FAPI controller for type-4 wind turbine units.

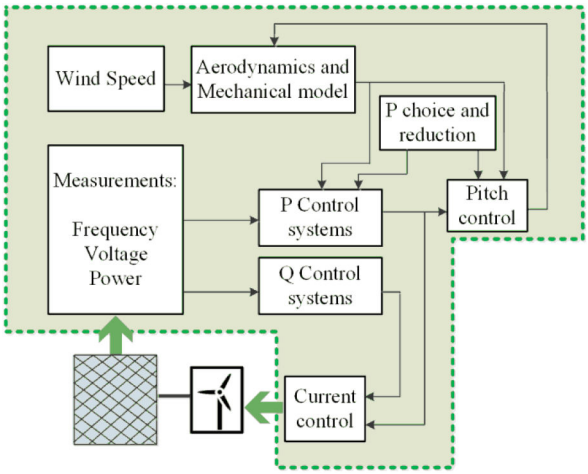

Fig. 1 *Control structure for the Type-4 wind generator*

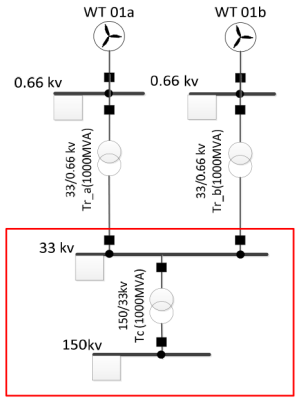

Fig. 2 *Grid-interface of a wind park with two types of WGs*

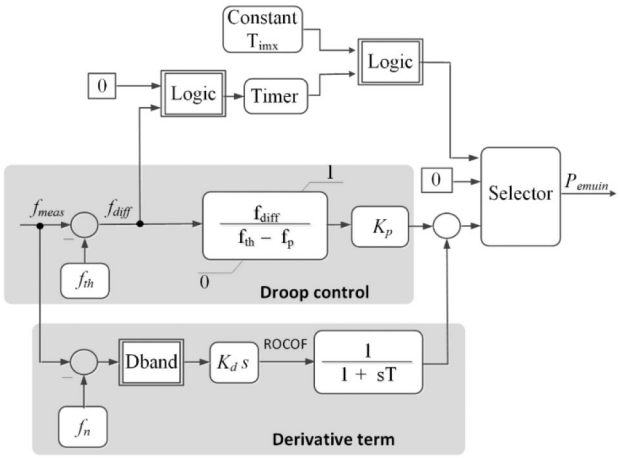

Fig. 3 *Block diagram of the derivative plus droop based FAPI controller used in Powerfactory*

Most of the existing reports on FAPI capabilities are focused on the proposition of different controllers which are mainly for a single WG unit or a small set of wind turbines which are linked to a small size test system. However, a comprehensive study on the influences of a given FAPI controller, its control gains, and the possible combination of wind generators that are facilitated by FAPI controllers are necessary for defining the maximum share of PEIG that does not bring risk on frequency instability. This paper addresses this gap by performing a sensitivity based methodology, based on time-domain simulations, to assess the influence of derivative-based FAPI control gains on the system frequency dynamics in the containment period. By evaluating individual and collective behaviour of PEIGs, an effective combination of wind generators with a FAPI controller and suitable settings for this controller will be pursued.

Since in both derivative and droop-based approaches, the input signal is the frequency error, therefore, the confident measurement of frequency in those methods is very important. It is worth to mention that the phase-locked loop (PLL) used for FAPI controller is different from the PLL used for the inner current control loop of voltage source converters. Thus, the dynamic performances of both PLL are different. Therefore, part of this paper is also devoted to assessing the impact of different values and parameter settings of the PLL used for the FAPI controller in a multi-machine interconnected power system. At the end of this paper, testing and validation of the proposed FAPI methods within EMT real-time simulations with proper recommendations are also performed to examine the implications on the generator and converters of a wind power generator type 4.

2 Fast active power injection for wind generation model

2.1 Wind generator model

This section provides an explanation about the main modified controllers of type IV (full converter interfaced) wind generator model, as developed in DigSILENT PowerFactory. The studied WG model is based on the standards of IEC 61400-27 series [7].

As shown in Fig. 1, the controller frame consists of input and measurement slots, the aerodynamic model, the main control slots, and the static generator slots.

In the measurement section of this model, the measurement blocks for frequency, power and voltage have a direct connection to the WG terminals. These measurement and also the currents which are coming from generator blocks are necessary for initialisation of the used model. The aerodynamic block is used for the representation of the mechanical parts of the WG unit. In this block, the mechanical power of the turbine is calculated. It is a single-mass component following the IEC 61400-27-1 standard [7].

The generator block consists of the 'static generator' from PowerFactory elements, and it will work as a controlled current source. The details of the Generator block are based on the IEC 61400-27-1 standard [25].

The P control and pitch angle controller blocks are built according to [25]. The 'FAPI controller' block, shown in light grey in Fig. 1, is an additional block for the developed WG model. Its input will be measured power or frequency, according to the implemented control approach, while its output is the additional reference to the active power control for FAPI capabilities.

As shown in Fig. 2, a wind park is implemented which can be used for representing the connection of various feeders with WGs.

2.2 Fast active power injection controller

In this paper, for adding the capability of inertia emulation to the model of WG, a detailed controller with the combination of droop and derivative techniques is designed and implemented. As shown in Fig. 3, the droop control loop injection/extraction of the active power can be changed according to the deviation of measured frequency from its nominal value (50/60 Hz). While within the derivative control loop, considering the control law in (1), a complementary action for FAPI can be performed.

$$\Delta P_{\text{emuin}} = -K_{\text{d}}\frac{\text{d}(\Delta f)}{\text{d}t} \tag{1}$$

The input signal of the proposed FAPI controller is the frequency deviation, and its output is the additional power that is added to the active power reference of the wind turbine controller. The required energy for this supplementary power is taken from the rotating masses of the WG or from the embedded additional energy in the DC link.

The main control parameters of this FAPI controller that affect the dynamic response during activation of the controller are the activation threshold for the FAPI controller (f_{th}), the maximum duration of FAPI activation (T_{imx}), the threshold for maximum

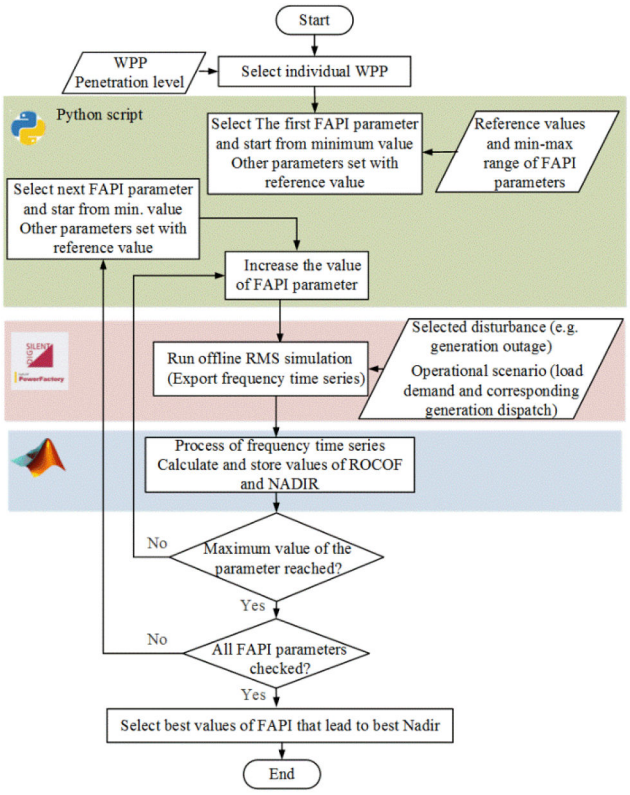

Fig. 4 *Procedure for tuning of the FAPI parameters*

emulated power (f_p), the allowable additional power output (K_p) and parameters of the derivative loop: the derivative gain (K_d) and the filter time constant (T). The value of f_{th} is assumed to be equal to 49.85 Hz. In case the frequency reaches an even lower value, corresponding with a second threshold f_p, then, the maximal allowed power through emulated inertia is released.

From Fig. 3, (see loop in the middle of the block diagram), it can be inferred that there is a linear dependence between frequency and the additional power signal (P_{emuin}), when the frequency deviation is between 1 and 0. During this interval, the following formula is used:

$$P_{emuin}(t) = \frac{f_{th} - f_{meas}(t)}{f_{th} - f_p} K_p \quad (2)$$

The value of K_p is assumed to be set between 10 and 25% of the nominal wind turbine active power [7, 23].

By using the tuning methodology presented in Section 3, the impact of each parameter considering the most suitable values can be analysed.

3 Sensitivity-based methodology for FAPI controller

The FAPI controller, explained in Section 2, is evaluated to determine the possible increase of the share of PEIG that can be achieved in the grid without jeopardising frequency stability.

The proposed sensitivity-based approach for tuning the FAPI controller's parameters located in selected wind power plants are presented in Fig. 4. This process will be used for a given test grid with several wind units for a given penetration level. For enabling this process the primary values of the FAPI control parameters for a given contingency, a given peal load with generation dispatches for a selected operational scenario and the network topology are necessary. Then, for each single wind generator which is facilitated with the FAPI controller, an automatic procedure (using the Python platform) is implemented to sweep over the parameters of the FAPI controller. As shown in Fig. 4, a time-domain simulation can be executed for extracting time data series, e.g. grid frequency, for more analysis in Matlab software. A Matlab script is used to evaluate the dynamics of the grid, e.g. calculation of Nadir for the selected operational scenario. The main goal here is to find a set of suitable values for FAPI parameters which can improve the FFR capabilities of the WG. The automatic procedure is performed for tuning each single WG unit. After that, a new operational scenario with a higher share of wind power can be selected and re-tuned by applying the same iteration considering various combinations between the wind parks. At the end of the procedure, the maximum share of WG with the most suitable combination can be found when the Nadir threshold cannot be met.

It should be noted that the parametric sensitivity approach is needed to first, qualitatively, check what kind of improvements and in which direction can be expected for RoCoF and Nadir within a possible range of FAPI parameters. Later, the optimisation approach can use the insights from the parametric sensitivity to define a suitable formulation and the necessary solver.

The objective here is to identify the value of each FAPI control parameter, which enhances the FFR of the wind power plant. This procedure is applied to the generic test system with three interconnected areas presented in [26]. To analyse the impact of the FAPI controller in a system configuration with a high share of wind power generation, a given different operational scenario is considered. The system with a 50% share of wind power generation was chosen as the starting point (base case).

As indicated in Fig. 4, RoCoF and Nadir are the main indicators for assessing frequency stability in the period of primary frequency control.

The RoCoF constitutes the frequency gradient after an imbalance event of active power generation and load demand. It is associated with the inertial response (0–300 ms from time of disturbance) according to the swing equation. Nadir corresponds to the lowest frequency value obtained after a power imbalance which depends on the system inertia, the response of the available frequency containment reserves, the size and location of the disturbance, and the pre-disturbance operating conditions. The criterion that defines the limit for NADIR is expressed as

$$f_{Nadir} \geq f_{min} \quad (3)$$

where f_{min} is the minimum acceptable frequency defined in the grid code.

This indicator has high relevance in the frequency control procedures because a low value (<47.5 Hz) might violate the security thresholds and a blackout can hardly be avoided due to the disconnection of generation units at this frequency.

It should be noted that DIgSILENT PowerFactory is a power system simulation program that has a dedicated application software interface (ASI) that enables the interconnection of several Python versions to execute various managing tasks (e.g. the modification of system's parameters in a particular power network). PowerFactory is already integrated with Python directly for automated calculations (e.g. parameter change, running simulations and import/export of data). This can also be done with Matlab, but the ASI used for that is much slower compared to the function used for direct communication with Python. Additionally, the use of Python as an open-source general programming language allows the interchange of information in real-time with other open-source or licensed programming languages (e.g. MATLAB), bringing in that way an interesting tool to utilise specialised methods (e.g. meta-heuristic optimisation function) for the power system stability analysis.

4 Case study for evaluation of the tuned controller

In this section, according to the explained procedure for parameter tuning of the FAPI controller in Section 3, the main parameters of the proposed controller are tuned and then the maximum share of wind power generation is identified. The implementation of the models and the benchmark system and the time-domain simulations are done by using DIgSILENT PowerFactory 2017. Several scripts were developed in Python 3.4 and Matlab R2016b

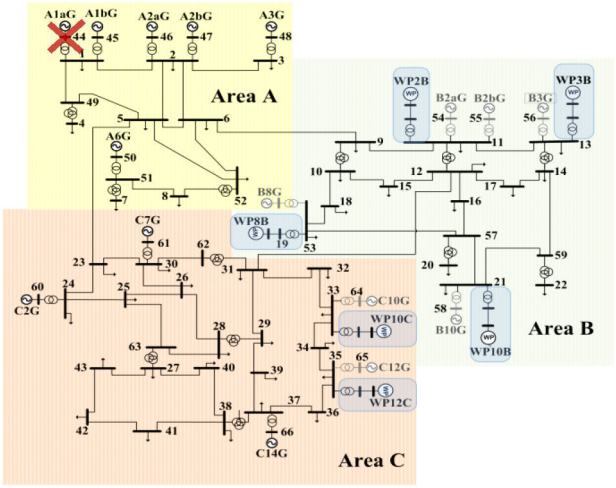

Fig. 5 *Three-area benchmark with WP integrations*

Table 1 Parameters of the FAPI controller for sensitivity analysis

Selected parameters	Value
f_{th}, Hz	49.90
f_p, Hz	49.75
K_p, pu	0.25
T_{imx},s	15
f_n, Hz	50
K_d, pu	10
T, s	0.25

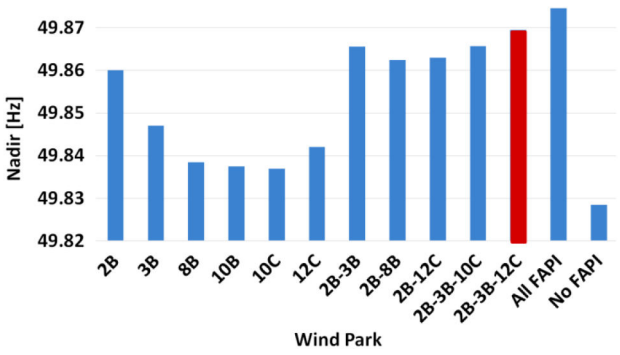

Fig. 6 *Nadir for different combinations of WP with FAPI controller*

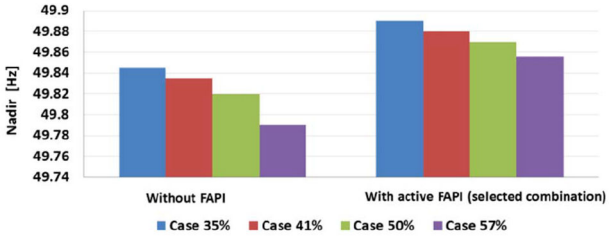

Fig. 7 *Nadir for different shares of wind power generation with and without droop-based FAPI controllers (three-area test system)*

to automate the FAPI parameter variations and the simulation of different operational scenarios and network topologies.

The single line diagram of the used generic test system (Section 3.2.3 of D1.2 [26]) is shown in Fig. 5, highlighting the added wind power plants, which are used to create different levels of a share of PEIG in the grid. A worst case of active power imbalance is created by considering the outage of the biggest synchronous generator (A1aG, which entails the loss of 1000 MW) for the winter load profile at $t = 5$ s. The total demand for the system is 15,480 MW.

As the base scenario, it is considered that 50% of the demand is supplied by wind power plants. Details of different operational scenarios, dispatches and system data are reported in D1.2 of the MIGRATE project [26]. After analysis and implementation of the proposed procedure in Fig. 4, the parameters used for parametric sensitivity-based tuning of the FAPI controller are given in Table 1. These set of values can be used for any combination of Wind Park used in the network.

5 Combination of multiple WP with FAPI controller

Ideally, it could be assumed that all wind power plants of a power system have an active FAPI controller. However, depending on the system characteristics, it might not be necessary to have all WPs with FAPI controller.

The size of the WP is the main key factor for implementing the FAPI. FAPI should be implemented in WPs which are large enough to facilitate the largest possible volume reserves for the FAPI controller to impact the grid. It is worth mentioning that, in addition to the size, the location of wind turbines with FAPI might be an alternative criterion for impacting the dynamic performance of the system. According to the finding in [27], it is better to have the PEIG units in proximity to low-inertia regions and far from the centre of inertia in the system. Furthermore, when the wind speed is low, the contribution of the FAPI controller (time duration and proportional gains) should be accordingly reduced in coherence with the available kinetic energy and if the speed is very low and below the rated operation, FAPI should not be activated to avoid stalling. A comprehensive study of all different factors of wind turbines that can affect the performance of any FAPI controller is discussed in [28].

Thus, it is worth evaluating if a minimum subset (combination) of wind power plants with FAPI can entail satisfactory frequency performance as in the case when all wind power plants perform with FAPI. Indeed, as shown in Fig. 6, the combination of WP2B, WP3B and WP12C has the highest and the most similar performance compared to the case that all the wind power plants actively perform FAPI.

6 Maximum share of PEIG in three area system

In this section, the effectiveness of the FAPI controller in increasing the share of wind power is evaluated. According to the ENTSO-E evaluation criteria, stationary values for Nadir between 49.8 and 50.2 Hz can be considered as the limits after the occurrence of an active power imbalance [29]. As shown in Fig. 7, within the existing controls, the maximum reachable share of PEIG level without FAPI controller is around 50% while after FAPI activation, with the best combination, it can be reached up to 57% for the three-area test system. The selected results that are shown in Fig. 7 correspond with the worst-case scenario (an outage of the largest generation unit in a heavily loaded condition). It has to be noted that 7% was an illustration for the most critical case, as defined on the MIGRATE project, in which the system has frequency instability in terms of grid codes limits without FAPI. So FAPI prevents instability and allows to increase the share a bit but keeping the existing grid codes [26].

In each studied method for each penetration level, the amounts of available reserves for primary frequency control are the same. It is concluded that by means of properly tuning of FAPI control in the key (selected) wind power plants, it is possible to ensure compliance of Nadir limit when increasing the share of wind power generation (which is a maximum 57% in case of the genetic test case 1).

It should be noted that the frequency threshold (e.g. Nadir) for defining the maximum penetration level in the studied three area test system has been considered according to continental Europe limits, while this can vary in different systems as reflected on their national grid codes. In this study, the penetration is considered as the amount of total demand covered by total generated wind power.

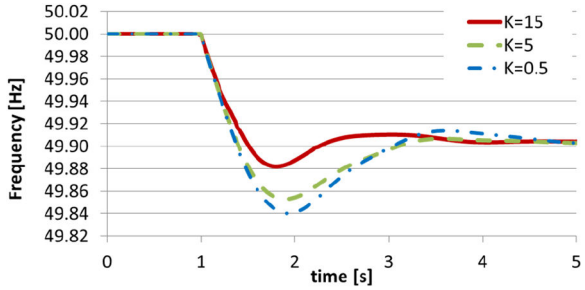

Fig. 8 *Frequency response for derivative-based FAPI controller*

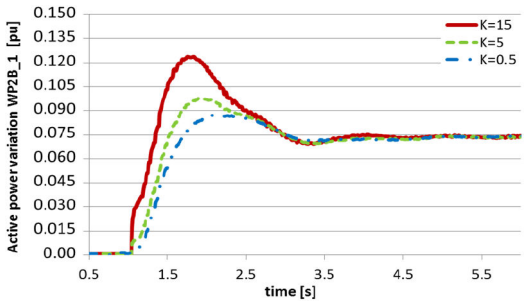

Fig. 9 *Variation of wind output power during FAPI activation (unit 1 of WP2B)*

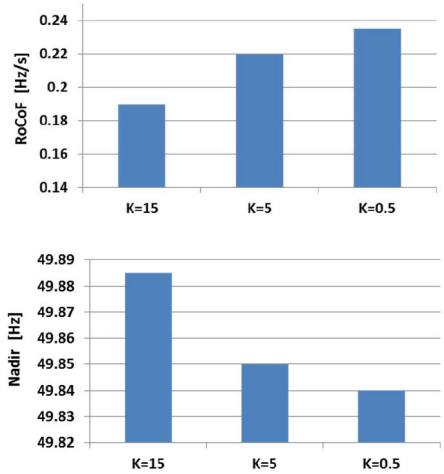

Fig. 10 *RoCoF and Nadir for derivative action of FAPI mitigation*

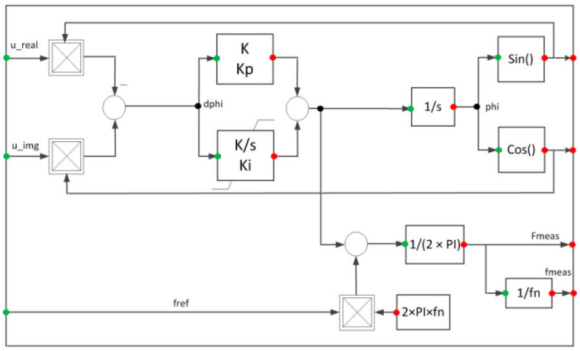

Fig. 11 *Standard model of a PLL in PowerFactory*

7 Test results of the derivative-based FAPI controller

Following the obtained results in previous sections, the proposed FAPI controller with derivative + droop term (shown in Fig. 3) is analysed with a generic test system with three areas. In the simulation scenario, the disturbance occurs at 1 s and parameters are the same as before. In this part of the simulation, secondary control is not modelled because the main focus of the study is devoted to primary frequency control.

The impact of the derivative-based FAPI controller for different values of the derivative control gain (K) is shown in Figs. 8–10, which indicates the mitigation of the frequency deviation after the occurrence of an active power imbalance.

As reported in [30], two sections of the curve of the frequency signal (measured in the period of primary frequency control) can be considered for the evaluation of the RoCoF. The first-time window is around 0.5 s from the time of occurrence of an active power imbalance, whereas the second time window lies between 0.5 and 2 s from the time of occurrence of an active power imbalance.

According to the obtained results in Fig. 8, the increase of the derivative gain entails an improvement of the frequency response, with an improvement of RoCoF in the time window of evaluation. For the sake of illustration, Fig. 9 shows the shape of the active power injection due to the action of the derivative-based FAPI controller attached to the largest wind generator of the system (see generator WP2B in Fig. 5).

From Figs. 8–10, it can be noted that a higher derivative gain causes a faster active power injection, leading to a higher influence on the frequency response. It should be noted that since in this case study the wind generators operate very close to their nominal output if the values of derivative gain became very high (comparing Figs. 8 and 9), it may lead to exceeding the allowed 10% margin above the nominal power. Hence, this margin should be considered as a bound for choosing the derivative gain.

It should be noted that FAPI is a generic control approach and different sources of energy can be used for providing the required energy for inertia emulation. This energy can be provided using stored energy within the DC link or mechanical part of the wind turbine. If the source of energy is a mechanical part, then the recovery strategy will be important. For example, as reported in [31] after the power increases, the WT will not be at the optimal operating speed. Therefore, the power decreases and according to the recovery control strategy, it is necessary to re-accelerate the generator. Such a recovery period may follow different strategies with several recovery times [32]. For such a case, time duration, amount of extracted power and minimum additional active power, activation duration, and allowed active power drop during the recovery period should be selected just as needed to ease the recovery for a wind turbine. To clarify these requirements, the IESO recently published a background document [33]. A detailed discussion on the limits and possible trade-off between consumed energy from the FAPI controller and the recovery time can be found in [28].

8 Impact of the PLL settings

A PLL is one of the methods commonly used for the synchronisation of grid-connected converters. The standard PLL library model of PowerFactory, which is used for generating the input signal of the FAPI block attached to the wind generator type-4, is presented in Fig. 11. In this model, the main parameters to be tuned are K_p and K_i [34]. A detailed description of the model of the PLL can be found on [34].

It is worth to mention that the PLL used for FAPI controller is different from the PLL used for the inner current control loop of voltage source converters. Thus, the dynamic performances of both PLLs are different. The dynamic response of the PLL for the inner current control loop of the converter should be considerably faster than the dynamics of the PLL used for FAPI controller, which should be selected according to the dynamic frequency response of the power system. In this section, the impact of different values and parameter settings of the PLL used for the FAPI controller is presented. As shown in Figs. 12 and 13, improper values of the gains can lead to slow or distorted signals which might bring instability when used as the input signals for FAPI controllers (in this test, the disturbance occurs at 5 s).

In these figures, the reference signal (f_reference) is the frequency of the reference machine in p.u and the impact of PLL control parameters can be observed on the estimated output signal

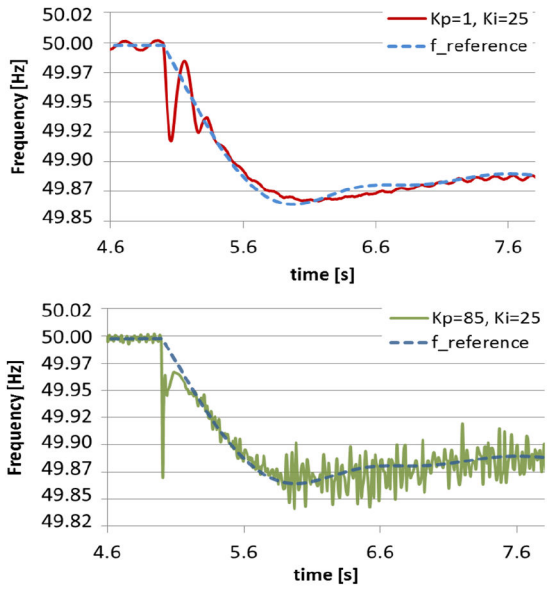

Fig. 12 *Impact of the setting of K_p on dynamics of the PLL*

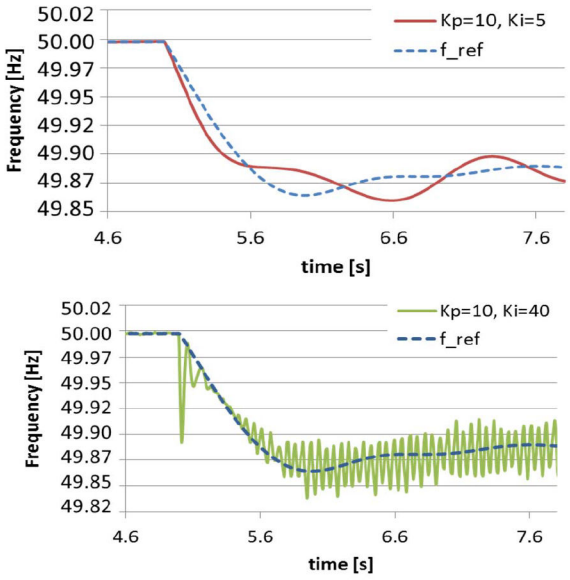

Fig. 13 *Impact of the setting of K_i on the PLL dynamics*

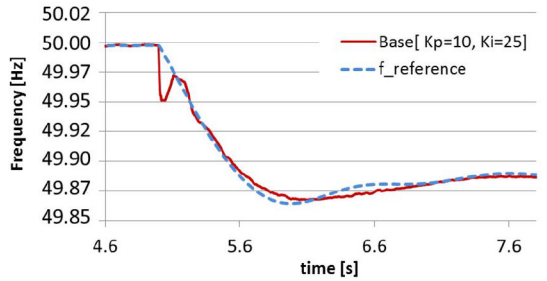

Fig. 14 *Performance of a tuned PLL for frequency stability analysis in PowerFactory*

which is going to be used by FAPI controller. The best performance is shown in Fig. 14 where the PLL can help to estimate the reference frequency in <150 ms without major inaccuracy, which is an acceptable time window for tracking the dynamics of the system's frequency.

Based on the presented results, the effects of the PLL can be explained as follows: when the PLL is too slow, the effectiveness of the derivative-based FAPI controller is lowered due to improper estimation of frequency in the required time window.

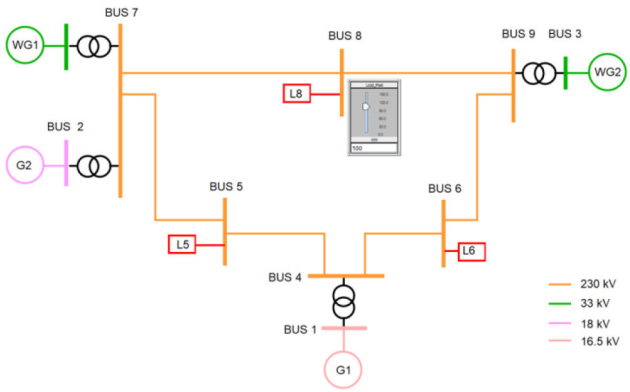

Fig. 15 *Generic test case-2 with added WG*

9 Validation with the real-time simulator

This section presents the design and implementation of the FAPI controller using an EMT test system build in a real-time digital simulator (RTDS) [35]. The test system is designed to represent specific critical situations, e.g. an operational scenario and electrical disturbance, which makes the system prone to frequency instability.

The EMT model of an interconnected power system is developed on RSCAD and running on RTDS NovaCor. RTDS allows external devices to be interfaced to the power system being simulated. The Software model for controlling the grid emulator and device under test (DUT) was developed by Triphase in Matlab/ Simulink environment, which is running on a real-time target (RTT) in real-time. RTT is a powerful, multi-core PC-based unit equipped with a real-time Linux/Xenomai-based operating system. A real-time inter-PC interface enables RTT to connect in real-time to the RTDS. The user has access and control on set-points of voltage and frequency of grid emulator and current set-points of DUT. RTT receives these set-points from RTDS. The Aurora communication protocol is used to exchange information between RTDS simulations and the RTT.

The EMT test system is based on the IEEE 9-bus test system, which is modified by adding two averaged EMT models of the wind generator Type 4 [25], which is a more detailed model of the RMS model shown in Fig. 2. The layout of the test system is shown in Fig. 15. Table 2 describes the load flow results in pre-disturbance conditions.

In this scenario, bus 8 was selected to create an under-frequency event (5% load increase) because the disturbance caused at this bus had the highest impact on Buses 3 and 7, where the wind turbines are connected. The droop based FAPI controllers should be activated when the frequency deviation is in the range of 0.06 to 0.1% of the nominal frequency value. As explained in Section 2, when $K_d = 0$, FAPI will act as a droop-based controller.

Fig. 16 depicts the frequency plots obtained for various proportional gains in reference to droop controller. As noticed from the figure, the case with $K_p = 0$ is the base plot where the FAPI controller is deactivated. As the value of K_p is increased, the influence of droop-based FAPI controller in frequency regulation increases, and as a result, Nadir improvement is witnessed. This can be corroborated in the plots of $K_p = 0.4, 0.5, 0.7$.

However, the further increase in K_p is leading to oscillations in frequency making the system behave as an under-damped system, causing a varying generation dispatch from wind generators. This is evident from the plots of $K_p = 1$ and 1.5.

Hence for $K_p = 0.7$, the best results were observed with a Nadir shift from 49.64 (base case) to 49.78 Hz which is an improvement of 38.88%.

This improvement is due to the FAPI from the DC side shown in Fig. 17, as the output of the FAPI controller of the WG unit, to compensate the frequency drop after the fault. In this case, the tuned value of the proportional gain is ~0.7. This value is obtained considering the physical limitation of the wind turbine for active power injecting <10% of its nominal power [7, 31].

Table 2 Load flow results from a test system with 52% wind share

Load flow results		*P*, MW	*Q*, MVAR
generations	G1	73.4	33.8
	WG1	82.6	0
	G1	78.2	−1.8
	WG2	84	0
loads	L5	125	50
	L6	90	30
	L8	100	35

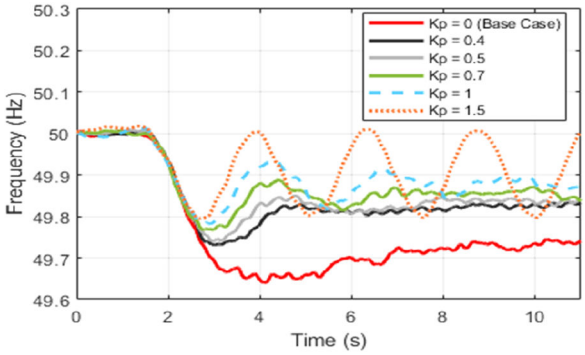

Fig. 16 *Frequency response due to load increase at bus 8 with proportional based FAPI controller at WG*

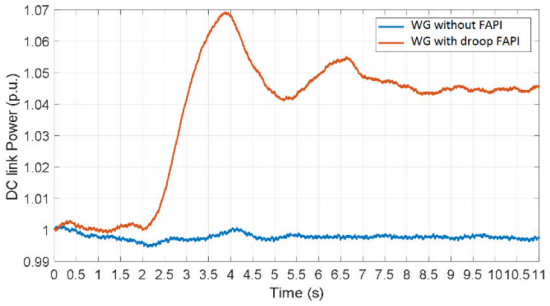

Fig. 17 *Response of the wind turbine for 5% load variation with 52% wind share with activated FAPI controller*

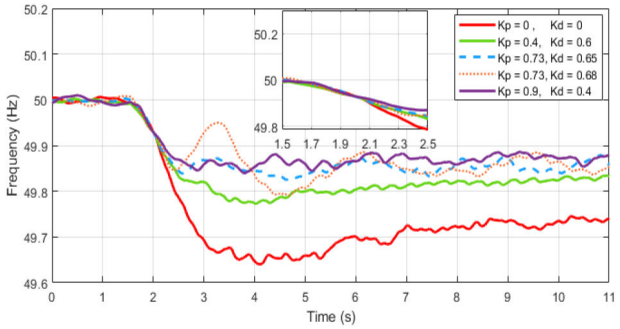

Fig. 18 *Frequency deviation with active derivative-based FAPI controller (load increase at bus 8)*

Fig. 18 depicts the frequency plots obtained for various values of proportional (K_p) and derivative gains (K_d) in reference to the derivative-based FAPI controller. The values selected here are the possible combinations of K_p and K_d achieved by careful tuning.

Here the plot with $K_p = 0$ and $K_d = 0$, forms the base plot with no derivative controller action. With $K_p = 0.4$ and $K_d = 0.6$, it can be observed that since K_p value is less, Nadir improvement is a comparatively lower but considerable improvement in dynamic frequency response before Nadir can be observed. A comparison between plots of $K_p = 0.73$, $K_d = 0.65$ and $K_p = 0.73$, $K_d = 0.68$ depicts also how sensitive the controller's behaviour is to the values

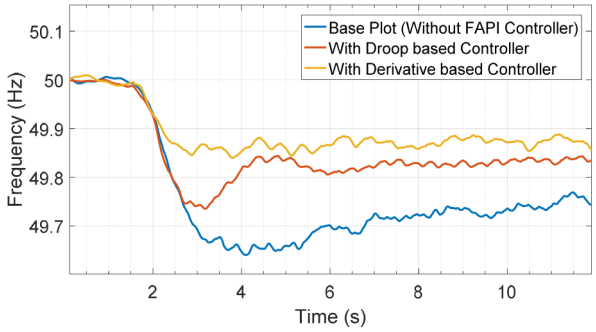

Fig. 19 *Frequency response due to load increase at Bus 8. (comparisons with different FAPI controllers)*

of the derivative controller gain (K_d), and consequently, the latter case shows the issues with under-damping which brings the oscillatory effect. At last, the plot with $K_p = 0.9$ and $K_d = 0.4$ gave the best results with RoCoF improvement from 280 mHz/s (base case) to 139.7 mHz/s accounting to 52% increase in RoCoF and Nadir shift from 49.64 (base case) to 49.845 Hz accounting to 58.3% increase in Nadir. RoCoF is calculated for a time window of 500 ms from 1.905 to 2.405 s after the time of dead-zone (~405 ms).

In summary, with the derivative-based FAPI controller, both Nadir and dynamic frequency response before Nadir could be improved by careful tuning of controller gains. Fig. 19 shows the comparison between the different FAPI controllers (droop-based and derivative-based controllers) that can be implemented in a Type-4 wind generator. The best plot from each of the controllers is taken to compare. From the obtained results, it can be noticed that the best performance is from the derivative-based FAPI controller which improves both Nadir and RoCoF.

10 Recommendation

- The recommended range for the activation threshold is around 49.95 Hz (which is aligned with findings reported in [36] that the permissible range of frequency change during steady state may be bounded up to ±0.05 Hz around the nominal value).
- Recommended thresholds for allowable additional power during activation of FAPI can be set from 10 to 25% of nominal power depending on the physical limitations in a wind power generator.
- The recommended range for the activation period is between 5 and 20 s, which is in line with the value reported in [7, 31, 37]. According to transmission system operators priorities, optimal management and coordination with other slower reserves and available sources of energy, the time duration for FAPI can be extended, considering underlying technical boundaries (e.g. due to recovery period for kinetic energy).
- Depending on available energy, according to the studies done in this work, the derivative gain can vary from 5 to 15. Due to the amplification of high-frequency noises, it is better to avoid using high values for the derivative gain. A low-pass filter with a time constant of ~0.25 s can be used to avoid this limitation [38].
- It is not necessary to choose bigger values for the low-pass filter time constant since it might impact the effectiveness of the controller by introducing a large delay. The gain should be selected such that it can reduce the impact of high-frequency noises.
- Different sources of energy such as ESSs, neighbour power reserve, and DC link can be used for further studies.
- Estimation of RoCoF as an input signal can help the performance of the frequency derivative-based FAPI controller. This can be confidently done by using emerging approaches, like a Kalman filter-based method shown in [39].
- Since the source of energy for the modified controller, in this part of the study, is the mechanical part of the wind turbine, then its performance will be limited with wind turbine physical

limits. This method can be also implemented by using ESSs to consider more flexibility.

11 Conclusions

A parametric sensitivity-based approach for evaluating the impacts of the proposed FAPI controller settings was proposed and applied into three area interconnected systems with a high share of wind power generation to ascertain how the parameters of the FAPI controllers can affect the dynamic frequency response of the system within the frequency containment period. From the presented case studies, recommended ranges for FAPI control parameters are provided. The values of these ranges do not apply to all systems due to the different dynamic properties of each power system. The parametric sensitivity-based approach can also be used as a tool to evaluate the maximum achievable share of power electronic interfaced renewable power generation. Other findings from the application of different FAPI controllers are summarised as follows:

- The activation threshold for the droop variant of FAPI control has a direct effect on the frequency Nadir.
- The proposed controller with derivative action is an effective solution for frequency containment mitigation. By using the proposed controller (combined methods of proportional + derivative technique), both Nadir and RoCoF values can be improved.

The derivative technique is dependent on the measurements derived from the PLL, and based on the performed analysis it was observed that improper settings (e.g. extremely low or high values for K_p or K_i) for PLL parameters might have a negative impact on the performance of the derivative-based FAPI controller.

12 Acknowledgments

This research was carried out as part of the MIGRATE project. This project has received funding from the European Union's Horizon 2020 research and innovation program under grant agreement No 691800. This paper reflects only the authors' views, and the European Commission is not responsible for any use that may be made of the information it contains.

13 References

[1] Gomez-Exposito, A., Conejo, A.J., Cañizares, C.: '*Electric energy systems: analysis and operation*' (CRC Press, Boca Raton, FL, USA, 2008)

[2] Rakhshani, E., Gusain, D., Sewdien, V., *et al.*: 'A key performance indicator to assess the frequency stability of converter dominated power system', *IEEE Access*, 2019, **7**, pp. 130957–130969

[3] Gu, H., Yan, R., Saha, T.K.: 'Minimum synchronous inertia requirement of renewable power systems', *IEEE Trans. Power Syst.*, 2018, **33**, (2), pp. 1533–1543

[4] Poolla, B.K., Groß, D., Dörfler, F.: 'Placement and implementation of grid-forming and grid-following virtual inertia and fast frequency response', *IEEE Trans. Power Syst.*, 2019, **34**, (4), pp. 3035–3046

[5] Mortazavi, H., Mehrjerdi, H., Saad, M., *et al.*: 'A monitoring technique for reversed power flow detection with high PV penetration level', *IEEE Trans. Smart Grid*, 2015, **6**, (5), pp. 2221–2232

[6] Adrees, A., Milanović, J.V., Mancarella, P.: 'Effect of inertia heterogeneity on frequency dynamics of low-inertia power systems', *IET Gener. Transm. Distrib.*, 2019, **13**, (14), pp. 2951–2958

[7] Engelken, S., Mendonca, A., Fischer, M.: 'Inertial response with improved variable recovery behaviour provided by type 4 WTs', *IET Renew. Power Gener. Spec.*, 2017, **11**, (3), pp. 195–201

[8] Dreidy, M., Mokhlis, H., Mekhilef, S.: 'Inertia response and frequency control techniques for renewable energy sources: a review', *Renew. Sustain. Energy Rev.*, 2017, **69**, (July 2016), pp. 144–155

[9] Ha, F., Abdennour, A.: 'Optimal use of kinetic energy for the inertial support from variable speed wind turbines', *Renew. Energy*, 2015, **80**, pp. 629–643

[10] Mishra, S., Zarina, P.P.: 'A novel controller for frequency regulation in a hybrid system with high PV penetration'. 2013 IEEE Power & Energy Society General Meeting, Vancouver, BC, 2013, pp. 1–5

[11] Yao, W., Lee, K.Y.: 'A control configuration of wind farm for load-following and frequency support by considering the inertia issue'. IEEE Power and Energy Society General Meeting, San Diego, CA, 2011, pp. 1–6

[12] Rakhshani, E., Rodriguez, P.: 'Inertia emulation in AC/DC interconnected power', *IEEE Trans. Power Syst.*, 2017, **32**, (5), pp. 3338–3351

[13] Gonzalez-Longatt, F., Chikuni, E., Rashayi, E.: 'Effects of the synthetic inertia from wind power on the total system inertia after a frequency disturbance'. IEEE Int. Conf. on Industrial Technology (ICIT), Cape Town, 2013, pp. 826–832

[14] Ackermann, T.: '*Wind power in power systems*', (John Wiley & Sons, Ltd, Chichester, UK, 2005)

[15] Rakhshani, E., Remon, D., Cantarellas, A.M., *et al.*: 'Virtual synchronous power strategy for multiple power systems', *IEEE Trans. Power Syst.*, 2017, **32**, (3), pp. 1665–1677

[16] Zhong, Q., Member, S., Weiss, G.: 'Synchronverters: inverters that mimic synchronous generators', *IEEE Trans. Ind. Electron.*, 2011, **58**, (4), pp. 1259–1267

[17] Liu, J., Tang, F., Zhao, J., *et al.*: 'Coherency identification for wind-integrated power system using virtual synchronous motion equation', *IEEE Trans. Power Syst.*, 2020, **35**, (4), pp. 2619–2630

[18] Zeng, X., Liu, T., Wang, S., *et al.*: 'Coordinated control of MMC-HVDC system with offshore wind farm for providing emulated inertia support', *IET Renew. Power Gener.*, 2020, **14**, (5), pp. 673–683

[19] Akram, U., Nadarajah, M., Raza, M.Q., *et al.*: 'Rocof restrictive planning framework and wind speed forecast informed operation strategy of energy storage system', *IEEE Trans. Power Syst.*, 2021, **36**, (1), pp. 224–234

[20] Xiong, L., Li, P., Wu, F., *et al.*: 'Stability enhancement of power systems with high DFIG-wind turbine penetration via virtual inertia planning', *IEEE Trans. Power Syst.*, 2019, **34**, (2), pp. 1352–1361

[21] Fernández-Guillamón, A., Vigueras-Rodríguez, A., Molina-García, Á.: 'Analysis of power system inertia estimation in high wind power plant integration scenarios', *IET Renew. Power Gener.*, 2019, **13**, (15), pp. 2807–2816

[22] Lin, W., Yin, Y.: 'Enhancing frequency response control by DFIGs in the high wind penetrated power systems', *IEEE Trans. Power Syst.*, 2011, **26**, (2), pp. 710–718

[23] Miao, Z., Member, S., Fan, L., *et al.*: 'Wind farms with HVdc delivery in inertial response and primary frequency control', *IEEE Trans. Energy Convers.*, 2010, **25**, (4), pp. 1171–1178

[24] Eriksson, R., Modig, N., Elkington, K.: 'Synthetic inertia versus fast frequency response: a definition', *IET Renew. Power Gener.*, 2018, **12**, (5), pp. 507–514

[25] Energynautics: 'MIGRATE project, type-3 and type-4 EMT – model documentation', Germany, 2017

[26] MIGRATE Work package 1: 'MIGRATE deliverable D1.2: report on power system analysis and key performance indicators', MIGRATE consortium, 2018. Available at www.h2020-migrate.eu

[27] Pulgar-Painemal, H., Wang, Y., Silva-Saravia, H.: 'On inertia distribution, inter-area oscillations and location of electronically-interfaced resources', *IEEE Trans. Power Syst.*, 2018, **33**, (1), pp. 995–1003

[28] Nikolopoulou, A.: 'Wind turbine contribution to ancillary services under increased renewable penetration levels'. MSc thesis, Delft University of Technology, 2017

[29] ENTSO-E: '*Continental Europe operation handbook – appendix 1: load-frequency control and performance*' (Brussels, 2009). Available at https://www.entsoe.eu/fileadmin/user_upload/_library/publications/entsoe/Operation_Handbook/Policy_1_final.pdf

[30] ENTSO-E: 'Rate of change of frequency (ROCOF) withstand capability', Brussels, 2018. Available at https://docstore.entsoe.eu/Documents/Network%20codes%20documents/NC%20RfG/IGD_RoCoF_withstand_capability_final.pdf

[31] Morren, J., Member, S., De Haan, S.W.H., *et al.*: 'Wind turbines emulating inertia and supporting primary frequency control', *IEEE Trans. Power Syst.*, 2006, **21**, (1), pp. 2005–2006

[32] Bossanyi, E.: 'Generic grid frequency response capability for wind power plant'. EWEA Annual Conf., France, Paris, November 2015

[33] 'LRP I RFP backgrounder – connection, March 10, 2015'. Available at http://www.ieso.ca/documents/generation-procurement/lrp/lrp-1-final/LRP-IRFP-Backgrounder-Connection.pdf, accessed 1 April 2016

[34] DIgSILENT: 'DIgSILENT PowerFactory technical reference documentation phase measurement device ElmPhi pll', Germany, 2016

[35] Simulation modelling libraries, RTDS Technologies Inc.

[36] Oak Ridge National Laboratory: '*Frequency control concerns in the North American electric power system*' (Tennessee, USA, 2002). Available at https://info.ornl.gov/sites/publications/Files/Pub57419.pdf

[37] ENTSO-E: '*Need for synthetic inertia (SI) for frequency regulation*' (Brussels, 2018). Available at https://docstore.entsoe.eu/Documents/Network%20codes%20documents/NC%20RfG/IGD_Need_for_Synthetic_Inertia_final.pdf

[38] Björnstedt, J.: 'Integration of non-synchronous generation'. Doctroal Thesis, Lund University, 2012

[39] Singh, A.K., Pal, B.C.: 'Rate of change of frequency estimation for power systems using interpolated DFT and kalman filter', *IEEE Trans. Power Syst.*, 2019, **34**, (4), pp. 1–1